# An accurate two-node finite element for the pre-twisted beam modelling

SAID ABID[1], MOHAMED TAKTAK[2*], FAKHREDDINE DAMMAK[2], MOHAMED HADDAR[2]

In this paper the development of a two-node finite element for the pre--twisted beam modelling is presented. This element is based on the mixed--hybrid formulation where the equilibrium equations are satisfied. Shear effects are taken into account in this formulation. Only one element can simulate the total behaviour of the beam. This element gives a good solution at nodes for the twisted beam problem. To illustrate the good performance of the proposed element, a comparison with other results from the literature is presented. Distribution of resulting forces along the beam is also presented for different load cases.

K e y w o r d s: pre-twisted beam, finite element, mixed-hybrid formulation, resulting forces

## 1. Introduction

The study of the pre-twisted beam behaviour is of great importance because of its use in many mechanical and civil engineering applications (vehicle structures, helicopter and boats helix, aircraft, propellers, compressor and turbine blades, plane engines, bridges, buildings, metallic edifices, satellite booms ...). The beam is considered pre-twisted if, in the stress-free state, the cross-section of the beam rotates relative to the end cross-section along the length of the beam. Among first researchers, who investigated the structure, we can mention Washizu [1] who presented an approximation theory for the beam under complicated loads and derived a system of governing equations of the structure. Because of the complexity of such equations, their solutions, with torsion, warping and transverse shear deformation effects taken into account, have not been found yet. Recently, Aimin et al. [2] and Yu et al. [3] treated the same problem and solved it using an analytical method to

[1] Unit of Mechanics, Modelling and Manufacturing, Preparatory Institute of Engineering Studies at Sfax Route Menzel Chaker K 0.5, 3018 Sfax, Tunisia

[2] Unit of Mechanics, Modelling and Manufacturing, Mechanical Engineering Department National School of Engineers of Sfax BP. N° W-3038 Sfax, Tunisia

[*] Corresponding author, e-mail address: mohamed.taktak@utc.fr

calculate displacements and stress of the structure subjected to different types of loads.

Another evidence of the importance of this kind of structure is its usefulness for finite element developers. In fact, it represents an excellent test to verify the accuracy of developed element and whether it is capable or not to take into account the initially non-planar configuration of the beam.

Although the problem of the pre-twisted beam is originally a beam problem, the element has rarely been used by beam elements developers. It has been especially used by the shell and 3D-elements developers. In fact, this structure, which is similar to a helicoidal shell with respect to surface geometry, is used by shell elements developers [4–28] to assess the effect of warping distortion on the performance of the shell element, also it represents a good test for membrane locking and evaluation of the ability of these shell elements to handle the double curvature geometries. In the case of a very thin plate, this problem will also underline the sensitivity of shell elements to both shear and membrane locking. Recently, this problem has been used to validate 3-D elements [29–36]. In recent works [37–40], authors proposed solutions for the pre-twisted beam with beam finite elements based on the geometrically exact finite-strain beam theory: governing equations of the beam element are derived with strain vectors which are the only unknown functions. Strains are derived in such a way that the relationship between displacements, strains and stress resultants is consistent with the virtual work principle.

All of these elements were tested through standard test suggested by MacNeal and Harder [19] and Simo et al. [28]: it consists of a clamped beam twisted 90° subjected to different load cases at the free end (in-plane and out-of-plane loads), the reference solution of this problem, based on the beam theory, was presented with and without shear effect.

In this paper, we propose a beam element that gives a good solution for the twisted beam problem with one element only. This element is based on a mixed--hybrid formulation where the equilibrium equations are satisfied. Shear effects are taken into account in the formulation. The accuracy of this formulation was tested by Taktak et al. [41] and Dammak et al. [42]. The outline of the paper is as follows: In section 2, we present geometric and kinematic descriptions of the twisted beam problem. The associated finite element is described in section 3. Finally, in section 4 we propose some solutions for the twisted beam problem obtained from beam, shell and 3-D elements. We show that the performance of the proposed element is clearly superior to the other presented elements.

## 2. Formulation

### 2.1 Geometric description

The beam under consideration is presented in Fig. 1: it is a gradually twisted beam defined in the global coordinate system $(O, X, Y, Z)$ of the global base

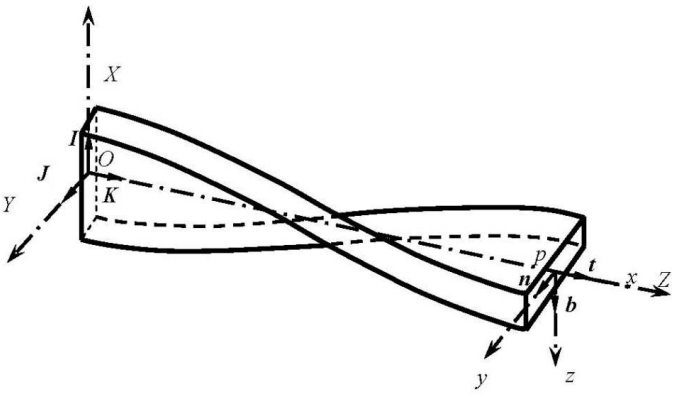


Fig. 1. Geometric description of the pre-twisted beam.

$(\boldsymbol{I}, \boldsymbol{J}, \boldsymbol{K})$ and generated by a succession of plane domains which are orthogonal to the axis $(OZ)$. Between two successive sections an angular difference exists which gives to the beam its helical form.

This beam is characterized by its width $l$, thickness $h$, length $L$ and the pitch $P$, which corresponds to the pitch of helical aspect of the beam. We suppose that sections are identical along the axis $(OZ)$. The middle fibre of this beam is linear and it coincides with the global axis $(OZ)$. For each point $p$ belonging to this line, we define the local coordinate system $(p, x, y, z)$ with its base $(\boldsymbol{t}, \boldsymbol{n}, \boldsymbol{b})$ defined by:

$$\boldsymbol{t} = \boldsymbol{K}, \qquad \boldsymbol{n} = \cos\theta \boldsymbol{I} + \sin\theta \boldsymbol{J}, \qquad \boldsymbol{b} = -\sin\theta \boldsymbol{I} + \cos\theta \boldsymbol{J}, \tag{1}$$

where $\theta$ is the twist angle: it is the angle between the projection of the axis $(py)$ in the plane $(OXY)$ and the axis $(OX)$.

The centroidal axis $x$ is straight at the beginning, but cross-sections are twisted about this axis. The linear relation between the local coordinate $x$ and the twist angle $\theta$ is shown by the following expression:

$$x = \rho\theta, \qquad \rho = \frac{P}{2\pi}. \tag{2}$$

The curvature radius $R$ and the torsion radius $T$ are defined as:

$$\frac{1}{R} = \left\| \frac{\mathrm{d}\boldsymbol{t}}{\mathrm{d}x} \right\| = 0, \qquad T = \left\| \frac{\mathrm{d}\boldsymbol{b}}{\mathrm{d}x} \right\| = \frac{2\pi}{P} \left\| \frac{\mathrm{d}\boldsymbol{b}}{\mathrm{d}\theta} \right\| = \frac{P}{2\pi}. \tag{3}$$

### 2.2 Kinematic description

In this study, we take into account the transverse shear strain and we suppose that the strain of the structure takes place such that the cross-section remains plane. Also we suppose that the torsion is uniform along the beam: all sections undergo the same warping.

For a point $p$ located in the middle fibre of the twisted beam, the virtual displacement vector expressed in the local coordinate system is given by the following expression:

$$\boldsymbol{u}_{\mathrm{p}}^{*} = u^{*}\boldsymbol{t} + v^{*}\boldsymbol{n} + w^{*}\boldsymbol{b}, \tag{4}$$

where $u^{*}$, $v^{*}$ and $w^{*}$ are virtual displacements parallel to $\boldsymbol{t}$, $\boldsymbol{n}$ and $\boldsymbol{b}$ vectors.

For a point $q$ different of $p$, belonging to the same section but not to the middle fibre, the corresponding virtual displacements vector is given by:

$$\boldsymbol{u}_{\mathrm{q}}^{*} = \boldsymbol{u}_{\mathrm{p}}^{*} + \boldsymbol{\theta}^{*} \wedge \boldsymbol{r}, \qquad \boldsymbol{r} = y\boldsymbol{n} + z\boldsymbol{b}, \tag{5}$$

$$\boldsymbol{\theta}^{*} = \theta_{\mathrm{t}}^{*}\boldsymbol{t} + \theta_{\mathrm{n}}^{*}\boldsymbol{n} + \theta_{\mathrm{b}}^{*}\boldsymbol{b}. \tag{6}$$

Expression (6) presents the vector of virtual rotations of the point $p$ composed of $\theta_{\mathrm{t}}^{*}$, $\theta_{\mathrm{n}}^{*}$ and $\theta_{\mathrm{b}}^{*}$ rotations around $\boldsymbol{t}$, $\boldsymbol{n}$ and $\boldsymbol{b}$ vectors, respectively.

The virtual displacement field gives three non-nil components of virtual strains which are the virtual axial strain $\varepsilon_{\mathrm{t}}^{*}$ and two virtual transverse shear strains $\gamma_{\mathrm{n}}^{*}$ and $\gamma_{\mathrm{b}}^{*}$ defined by Bouabdallah [43]:

$$\varepsilon_{\mathrm{t}}^{*} = \varepsilon_{\mathrm{tt}}^{*} = e_{\mathrm{t}}^{*} - y\chi_{\mathrm{b}}^{*} + z\chi_{\mathrm{n}}^{*}, \tag{7}$$

$$\gamma_{\mathrm{n}}^{*} = 2\varepsilon_{\mathrm{nt}}^{*} = \gamma_{\mathrm{tn}}^{*} - z\chi_{\mathrm{t}}^{*}, \tag{8}$$

$$\gamma_{\mathrm{b}}^{*} = 2\varepsilon_{\mathrm{bt}}^{*} = \gamma_{\mathrm{tb}}^{*} - y\chi_{\mathrm{t}}^{*}, \tag{9}$$

$e_{\mathrm{t}}^{*}$ is the virtual membrane strain, $\gamma_{\mathrm{tn}}^{*}$ and $\gamma_{\mathrm{tb}}^{*}$ are virtual shear strains defined as:

$$e_{\mathrm{t}}^{*} = \frac{1}{\rho}\frac{\mathrm{d}u^{*}}{\mathrm{d}\theta}, \tag{10}$$

$$\gamma_{\mathrm{tn}}^{*} = \frac{1}{\rho}\left(\frac{\mathrm{d}v^{*}}{\mathrm{d}\theta} - \delta w\right) - \delta\theta_{\mathrm{b}}^{*}, \tag{11}$$

$$\gamma_{\mathrm{tb}}^{*} = \frac{1}{\rho}\left(\frac{\mathrm{d}w^{*}}{\mathrm{d}\theta} - \delta v\right) + \theta_{\mathrm{n}}^{*}, \tag{12}$$

$\chi_{\mathrm{t}}^*$, $\chi_{\mathrm{n}}^*$, $\chi_{\mathrm{b}}^*$ are virtual curvatures in planes $(p, y, z)$, $(p, x, z)$ and $(p, y, x)$ presented as:

$$\chi_{\mathrm{t}}^* = \frac{1}{\rho}\frac{\mathrm{d}\theta_{\mathrm{t}}^*}{\mathrm{d}\theta}, \tag{13}$$

$$\chi_{\mathrm{n}}^* = \frac{1}{\rho}\left(\frac{\mathrm{d}\theta_{\mathrm{n}}^*}{\mathrm{d}\theta} - \theta_{\mathrm{b}}^*\right), \tag{14}$$

$$\chi_{\mathrm{b}}^* = \frac{1}{\rho}\left(\frac{\mathrm{d}\theta_{\mathrm{b}}^*}{\mathrm{d}\theta} - \theta_{\mathrm{n}}^*\right). \tag{15}$$

These strains form the vector of virtual generalized strains:

$$\langle \varepsilon^* \rangle = \langle e_{\mathrm{t}}^* \quad \gamma_{\mathrm{tn}}^* \quad \gamma_{\mathrm{tb}}^* \quad \chi_{\mathrm{t}}^* \quad \chi_{\mathrm{n}}^* \quad \chi_{\mathrm{b}}^* \rangle. \tag{16}$$

From the beam theory, static equilibrium equations of this type of beam are written in the local coordinate system as:

$$\begin{cases} \dfrac{\mathrm{d}N}{\mathrm{d}\theta} = 0 \\ \dfrac{\mathrm{d}T_{\mathrm{n}}}{\mathrm{d}\theta} - T_{\mathrm{b}} = 0 \\ T_{\mathrm{n}} + \dfrac{\mathrm{d}T_{\mathrm{b}}}{\mathrm{d}\theta} = 0 \end{cases} \qquad \begin{cases} \dfrac{\mathrm{d}M_{\mathrm{t}}}{\mathrm{d}\theta} = 0 \\ \dfrac{\mathrm{d}M_{\mathrm{n}}}{\mathrm{d}\theta} - M_{\mathrm{b}} - \dfrac{PT_{\mathrm{b}}}{2\pi} = 0 \\ M_{\mathrm{n}} + \dfrac{\mathrm{d}M_{\mathrm{b}}}{\mathrm{d}\theta} + \dfrac{PT_{\mathrm{n}}}{2\pi} = 0 \end{cases} \tag{17}$$

where $N$ is the axial force, $T_{\mathrm{n}}$ and $T_{\mathrm{b}}$ are normal and binormal shearing forces defined as:

$$N = \int_A \sigma_{\mathrm{t}} \mathrm{d}A, \qquad T_{\mathrm{n}} = \int_A \sigma_{\mathrm{tn}} \mathrm{d}A, \qquad T_{\mathrm{b}} = \int_A \sigma_{\mathrm{tb}} \mathrm{d}A \tag{18}$$

and $M_{\mathrm{t}}$ is the torsional moment, $M_{\mathrm{n}}$ and $M_{\mathrm{b}}$ are bending moments around the $(p, y)$ and $(p, z)$. They are defined as follows:

$$M_{\mathrm{t}} = \int_A (y\sigma_{\mathrm{tb}} - z\sigma_{\mathrm{tn}}) \mathrm{d}A, \qquad M_{\mathrm{n}} = \int_A z\sigma_{\mathrm{t}} \mathrm{d}A, \qquad M_{\mathrm{b}} = \int_A -y\sigma_{\mathrm{t}} \mathrm{d}A, \tag{19}$$

$\mathrm{d}A$ is an elementary surface of the beam cross-section. These forces constitute the vector of resulting forces:

$$\langle \boldsymbol{R} \rangle = \langle N \quad T_{\mathrm{n}} \quad T_{\mathrm{b}} \quad M_{\mathrm{t}} \quad M_{\mathrm{n}} \quad M_{\mathrm{b}} \rangle. \tag{20}$$

### 2.3 Constitutive behaviour

The beam has an isotropic material behaviour; stresses are related to strains by the following expressions:

$$\sigma_{\mathrm{t}} = E\varepsilon_{\mathrm{t}}, \qquad \sigma_{\mathrm{tn}} = G\gamma_{\mathrm{n}}, \qquad \sigma_{\mathrm{tb}} = G\gamma_{\mathrm{b}}, \tag{21}$$

$E$ and $G$ are the Young's and the shear modulus of the beam material, respectively.

Seen the shape of the section (rectangular cross-section), the local coordinate system $(p, x, y, z)$ is coincident with principal axes of inertia: axes $(pz)$ and $(py)$ are axes of symmetry of the rectangular cross-section. $\{\boldsymbol{R}\}$ is related to $\{\boldsymbol{\varepsilon}\}$ by the elastic behaviour matrix $[\boldsymbol{H}]$:

$$\{\boldsymbol{R}\} = [\boldsymbol{H}]\{\boldsymbol{\varepsilon}\}, \tag{22}$$

$$[\boldsymbol{H}] = \mathrm{diag}(EA, kGA, kGA, GJ, EI_y, EI_z), \tag{23}$$

$A$ is the section area, $J$ is the quadratic moment of torsion, $I_y$ and $I_z$ are central quadratic moments regarding $(p, y)$ and $(p, z)$ axes, $k$ is the shear correction factor for the rectangular section ($k = 0.883$). These parameters are defined by Batoz and Dhatt [44]:

$$\begin{aligned} J &= \frac{lh^3}{16}\left(\frac{16}{3} - \frac{37}{11}\frac{h}{l}\left(1 - \frac{1}{12}\left(\frac{h}{l}\right)^4\right)\right), \\ I_y &= \frac{1}{12}lh^3, \qquad I_z = \frac{1}{12}hl^3. \end{aligned} \tag{24}$$

## 3. Development of the finite element

The developed element is a two-node element, which simulates the total beam; each node corresponds to each extremity of the twisted structure. The mixed--hybrid formulation of energy associated to equilibrium equations and the stress--strain relation in the local coordinate system is expressed by Batoz and Dhatt [44]:

$$\Pi = \Pi_{\mathrm{int}} - \Pi_{\mathrm{ext}}, \tag{25}$$

$$\Pi_{\mathrm{int}} = \int_0^L \left(-\frac{1}{2}\langle\boldsymbol{R}\rangle[\boldsymbol{H}]^{-1}\{\boldsymbol{R}\} + \langle\boldsymbol{\varepsilon}\rangle\{\boldsymbol{R}\}\right)\mathrm{d}x, \tag{26}$$

$$\Pi_{\text{ext}} = \int_0^L \langle \boldsymbol{u} \rangle \{\boldsymbol{f}\} \mathrm{d}x + \left( \langle \boldsymbol{u} \rangle \{\boldsymbol{F}\} \right)_S , \tag{27}$$

$\langle \boldsymbol{u} \rangle$ is the vector of displacements, $\{\boldsymbol{f}\}$ is one of external distributed forces, $\{\boldsymbol{F}\}$ is the vector of external concentrated forces and $S$ is the beam boundary. The integration of the second term of the functional of internal energy gives:

$$\Pi_{\text{int}} = \int_0^L -\frac{1}{2} \langle \boldsymbol{R} \rangle [\boldsymbol{H}]^{-1} \{\boldsymbol{R}\} \mathrm{d}x + \langle \boldsymbol{u}_{\text{n}} \rangle \{\boldsymbol{R}_{\text{n}}\}, \tag{28}$$

$$\langle \boldsymbol{u}_{\text{n}} \rangle = \langle u_1 \quad v_1 \quad w_1 \quad \theta_{\text{t1}} \quad \theta_{\text{n1}} \quad \theta_{\text{b1}} \quad u_2 \quad v_2 \quad w_2 \quad \theta_{\text{t2}} \quad \theta_{\text{n2}} \quad \theta_{\text{b2}} \rangle, \tag{29}$$

$$\begin{aligned} \langle \boldsymbol{R}_{\text{n}} \rangle = \langle & -N_1 \quad -T_{\text{n1}} \quad -T_{\text{b1}} \quad -M_{\text{t1}} \quad -M_{\text{n1}} \quad -M_{\text{b1}} \\ & N_2 \quad T_{\text{n2}} \quad T_{\text{b2}} \quad M_{\text{t2}} \quad M_{\text{n2}} \quad M_{\text{b2}} \rangle, \end{aligned} \tag{30}$$

$\langle \boldsymbol{u}_{\text{n}} \rangle$ and $\langle \boldsymbol{R}_{\text{n}} \rangle$ represent vectors of nodal displacements and resulting forces, respectively. The expression of the virtual internal work of the beam is then written as (Batoz and Dhatt [44]):

$$W_{\text{int}} = \int_0^L -\langle \boldsymbol{R}^*_{\text{n}} \rangle [\boldsymbol{H}]^{-1} \{\boldsymbol{R}_{\text{n}}\} \mathrm{d}x + \langle \boldsymbol{u}^*_{\text{n}} \rangle \{\boldsymbol{R}_{\text{n}}\} + \langle \boldsymbol{R}^*_{\text{n}} \rangle \{\boldsymbol{u}_{\text{n}}\}, \tag{31}$$

"*" corresponds to the virtual value. The resolution of static equilibrium equations permits to express the vector $\{\boldsymbol{R}\}$ according to the vector of independent parameters $\{\boldsymbol{\alpha}_{\text{n}}\}$ with the following matrix form:

$$\{\boldsymbol{R}\} = [\boldsymbol{P}] \{\boldsymbol{\alpha}_{\text{n}}\}, \tag{32}$$

$$\langle \boldsymbol{\alpha}_{\text{n}} \rangle = \langle \alpha_1 \quad \alpha_2 \quad \alpha_3 \quad \alpha_4 \quad \alpha_5 \quad \alpha_6 \rangle. \tag{33}$$

This vector represents resulting forces on one of the two nodes of the element, $[\boldsymbol{P}]$ is the approximation matrix of resulting forces. This matrix is presented as:

$$[\boldsymbol{P}] = \begin{bmatrix} 1 & 0 & 0 & 0 & 0 & 0 \\ 0 & \cos\theta & -\sin\theta & 0 & 0 & 0 \\ 0 & -\sin\theta & -\cos\theta & 0 & 0 & 0 \\ 0 & 0 & 0 & 1 & 0 & 0 \\ 0 & -\rho\theta\sin\theta & -\rho\theta\cos\theta & 0 & -\cos\theta & \sin\theta \\ 0 & -\rho\theta\cos\theta & \rho\theta\sin\theta & 0 & \sin\theta & \cos\theta \end{bmatrix}. \tag{34}$$

$\langle \boldsymbol{R}_{\mathrm{n}} \rangle$ is related to $\{\boldsymbol{\alpha}_{\mathrm{n}}\}$ as:

$$\langle \boldsymbol{R}_{\mathrm{n}} \rangle = \{\boldsymbol{\alpha}_{\mathrm{n}}\}[\boldsymbol{A}], \tag{35}$$

$$[\boldsymbol{A}] = \left[-[\boldsymbol{P}_1]^{\mathrm{T}} M [\boldsymbol{P}_2]^{\mathrm{T}}\right], \tag{36}$$

$[\boldsymbol{P}_1]$ and $[\boldsymbol{P}_2]$ are approximation matrices calculated at the two ends of the beam. The expression of the virtual internal work can be written as:

$$W_{\mathrm{int}} = -\langle \boldsymbol{\alpha}^*_{\mathrm{n}} \rangle [\boldsymbol{B}] \{\boldsymbol{\alpha}_{\mathrm{n}}\} + \langle \boldsymbol{u}^*_{\mathrm{n}} \rangle [\boldsymbol{A}]^{\mathrm{T}} \{\boldsymbol{\alpha}_{\mathrm{n}}\} + \langle \boldsymbol{\alpha}^*_{\mathrm{n}} \rangle [\boldsymbol{A}] \{\boldsymbol{u}_{\mathrm{n}}\}, \tag{37}$$

$$[\boldsymbol{B}] = \int_0^L [\boldsymbol{P}]^{\mathrm{T}} [\boldsymbol{H}]^{-1} [\boldsymbol{P}] \mathrm{d}x. \tag{38}$$

After elimination of independent parameters, the virtual internal work of the system becomes:

$$W_{\mathrm{int}} = \langle \boldsymbol{u}^*_{\mathrm{n}} \rangle [\boldsymbol{k}] \{\boldsymbol{u}_{\mathrm{n}}\}, \tag{39}$$

$$[\boldsymbol{k}] = [\boldsymbol{A}]^{\mathrm{T}} [\boldsymbol{B}]^{-1} [\boldsymbol{A}], \tag{40}$$

where $[\boldsymbol{k}]$ is the local stiffness matrix. The global stiffness matrix is then defined as:

$$[\boldsymbol{K}] = [\boldsymbol{T}]^{\mathrm{T}} [\boldsymbol{k}]^{-1} [\boldsymbol{T}]. \tag{41}$$

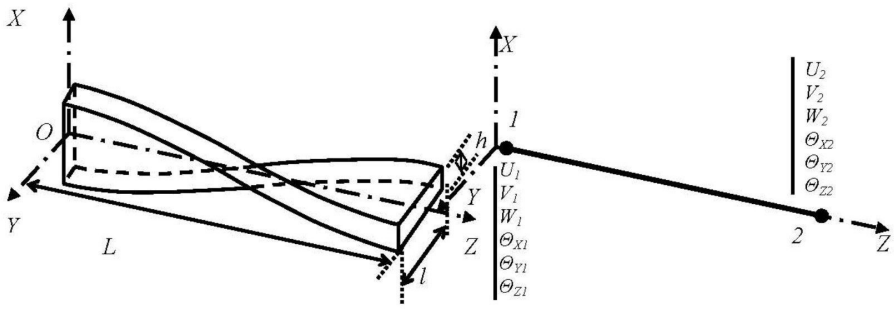


Fig. 2. Developed finite element.

T a b l e 1. In plane and out of plane deflections of the MacNeal and Harder problem

| Method | Refer. | Mesh | In plane | Normalized | Out of plane | Normalized |
|---|---|---|---|---|---|---|
| Analytical | [19] | | 0.005424 | | 0.001754 | |
| Solid-shell | [29] | 2×12 | 0.005587 | 1.030 | 0.001754 | 1.000 |
| elements | [31] | 6 × 2× 1 | 0.005387 | 0.993 | 0.001724 | 0.982 |
| | [33] | 12 × 4×12 | 0.005315 | 0.979 | 0.001721 | 0.981 |
| | | 12 × 4×24 | 0.005375 | 0.990 | 0.001742 | 0.993 |
| | | 12 × 4×48 | 0.005385 | 0.992 | 0.001744 | 0.994 |
| | | 12 × 4×96 | 0.005385 | 0.992 | 0.001744 | 0.994 |
| | [34] | 1× 6 | 0.005445 | 1.004 | 0.001755 | 1.001 |
| | | 2×12 | 0.005418 | 0.999 | 0.001748 | 0.997 |
| | [35] | 1× 6 | 0.005440 | 1.003 | 0.001755 | 1.001 |
| Shell | [6] | 2×12 | 0.005386 | 0.992 | 0.001731 | 0.986 |
| elements | | 4×24 | 0.005407 | 0.996 | 0.001746 | 0.995 |
| | | 6×36 | 0.005312 | 0.997 | 0.001749 | 0.997 |
| | [9] | 1× 6 | 0.005412 | 0.997 | 0.001747 | 0.996 |
| | | 2×12 | 0.005413 | 0.998 | 0.001751 | 0.998 |
| | [13] | 2×12 | 0.005405 | 0.996 | 0.001755 | 1.000 |
| | [14] | 1× 6 | 0.005407 | 0.996 | 0.001680 | 0.958 |
| | | 2×12 | 0.005412 | 0.997 | 0.001751 | 0.998 |
| | | 4×24 | 0.005412 | 0.997 | 0.001746 | 0.996 |
| | [15] | 6× 1 | 0.005390 | 0.993 | 0.001759 | 1.002 |
| | | 12× 2 | 0.005405 | 0.996 | 0.001754 | 1.000 |
| | | 24× 4 | 0.005411 | 0.997 | 0.001751 | 0.998 |
| | [16] | 2×12 | 0.005335 | 0.983 | 0.001719 | 0.980 |
| | | 8×48 | 0.005399 | 0.995 | 0.001749 | 0.997 |
| | [17] | 2×12 | 0.005566 | 1.026 | 0.001795 | 1.023 |
| | | 8×48 | 0.010502 | 1.936 | 0.002664 | 1.518 |
| | [18] | 2×12 | 0.005402 | 0.995 | 0.001753 | 0.999 |
| | | 8×48 | 0.005416 | 0.998 | 0.001751 | 0.998 |
| | [21] | 2×12 | 0.005439 | 1.003 | 0.001738 | 0.991 |
| | | 8×48 | 0.005411 | 0.998 | 0.001751 | 0.998 |
| | [24] | 1× 6 | 0.005358 | 0.988 | 0.001748 | 0.997 |
| | | 2×12 | 0.005418 | 0.999 | 0.001754 | 1.000 |
| | [25] | 3×13 | 0.005407 | 0.997 | 0.001746 | 0.996 |
| | | 5×25 | 0.005413 | 0.998 | 0.001752 | 0.999 |
| | [27] | 2×12 | 0.005397 | 0.995 | 0.001727 | 0.984 |
| | | 8×48 | 0.005416 | 0.998 | 0.001751 | 0.998 |
| Beam | [37] | 12 | 0.005402 | 0.995 | 0.001741 | 0.992 |
| elements | [38, 39, 40] $E_2$ | 1 | 0.005474 | 1.009 | 0.001517 | 0.978 |
| | | 2 | 0.005429 | 1.000 | 0.001738 | 0.990 |
| | | 3 | 0.005429 | 1.000 | 0.001748 | 0.996 |
| | | 6 | 0.005429 | 1.000 | 0.001750 | 0.997 |
| | | 12 | 0.005429 | 1.000 | 0.001750 | 0.997 |
| | [38, 39, 40] $E_3$ | 1 | 0.005422 | 0.999 | 0.001750 | 0.997 |
| | | 2 | 0.005429 | 1.000 | 0.001750 | 0.997 |
| | Present | 1 | 0.005429 | 1.000 | 0.001749 | 0.997 |
| | | 2 | 0.005429 | 1.000 | 0.001750 | 0.997 |
| | | 3 | 0.005429 | 1.000 | 0.001750 | 0.997 |

[$\boldsymbol{T}$] is the transfer matrix from the local coordinate system to the global one; it is defined by Eq. (1). Figure 2 presents the developed element according to the real description of the beam.

## 4. Numerical examples

*Example 1: MacNeal and Harder test*

This example is the standard test studied by Harder and MacNeal [19]: it deals with an elastic cantilever beam. Geometric and mechanical characteristics of the corresponding pre-twisted beam are: length $L = 12$; width $l = 1.1$, thickness $h = 0.32$, Young's modulus $E = 29 \times 10^6$ and Poisson coefficient $\nu = 0.22$. It is a non-dimensional test but in our study, we choose to express length values in [Length unit]. The undeformed free end of the beam is twisted by an angle of 90° in comparison to the clamped extremity, in which all nodal d.o.f.s are restrained. This beam is subjected to 1 N in-plane and out-of-plane force at its free end. Table 1 presents values of deflections in the two cases of load given by different finite elements as well as the finite element developed in this study. These results are normalized with respect to the analytical result presented by MacNeal and Harder [19] to compare the efficiency of these elements. Developed finite element presents

Table 2. Deflections of Simo Problem

| Method | Refer. | Mesh | Out plane force | | | In plane force | | |
|---|---|---|---|---|---|---|---|---|
| | | × | $U$ | $V$ | $W$ | $U$ | $V$ | $W$ |
| Analytical | [28] | | −0.3431 | | | | −1.3900 | |
| Shell element | [12] | 1× 6 | −0.3578 | | | | −1.4147 | |
| | | 2×12 | −0.3448 | | | | −1.3953 | |
| | | 2×24 | −0.3406 | | | | −1.3772 | |
| | | 4×48 | −0.3431 | | | | −1.3870 | |
| | [23] | 1× 6 | −0.3225 | | | | −1.3800 | |
| | | 2×12 | −0.3376 | | | | −1.3828 | |
| | | 2×24 | −0.3417 | | | | −1.3856 | |
| | | 4×48 | −0.3427 | | | | −1.3870 | |
| | [26] | 6× 1 | −0.3502 | | | | −1.3883 | |
| | | 12× 2 | −0.3464 | | | | −1.3897 | |
| | | 24× 4 | −0.3436 | | | | −1.3883 | |
| | | 48× 8 | −0.3430 | | | | −1.3870 | |
| | [28] | 6× 1 | −0.3261 | | | | −1.3786 | |
| | | 12× 2 | −0.3383 | | | | −1.3870 | |
| | | 24× 4 | −0.3421 | | | | −1.3890 | |
| | | 48× 8 | −0.3431 | | | | −1.3900 | |
| Solid-shell element | [32] | 12 × 1×1 | −0.1360 | −0.1848 | $0.1386\ 10^{-1}$ | −0.1848 | −0.3192 | $0.7964\ 10^{-8}$ |
| | | 12 × 2×2 | −0.1406 | −0.1911 | $-0.2997\ 10^{-12}$ | −0.1911 | −0.3284 | $-0.2432\ 10^{-1}$ |
| | | 12 × 4×2 | −0.1416 | −0.1925 | $-0.1627\ 10^{-11}$ | −0.1925 | −0.3305 | $0.2448\ 10^{-1}$ |
| | | 24 × 24×2 | −0.3070 | −0.4334 | $0.1624\ 10^{-11}$ | −0.4334 | −0.9536 | $0.3954\ 10^{-11}$ |
| | | 48 × 4×2 | −0.3314 | −0.4741 | $-0.6714\ 10^{-8}$ | −0.4741 | −1.2495 | $-0.6416\ 10^{-8}$ |
| Present | | 1 | −0.3427 | −0.4912 | 0 | −0.4912 | −1.394 | 0 |
| | | 2 | −0.3427 | −0.4912 | 0 | −0.4912 | −1.394 | 0 |
| | | 3 | −0.3427 | −0.4912 | 0 | −0.4912 | −1.394 | 0 |

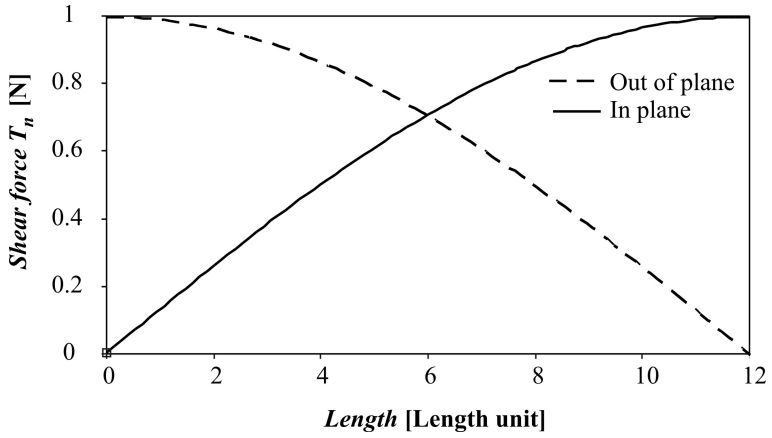


Fig. 3. Distribution of the module of the shear force $T_{\mathrm{n}}$.

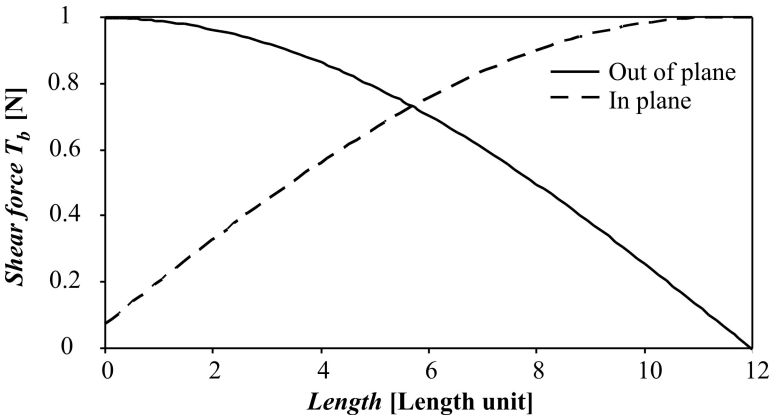


Fig. 4. Distribution of the module of the shear force $T_{\mathrm{b}}$.

good results in the two studied cases of load and the accuracy of the developed element is independent on the finite element mesh: only one of the developed elements suffices to obtain displacements which correspond to those obtained by the analytical solution despite the complexity of the form, whereas other beam element requires at least 2 elements to converge. The other model (3-D finite element, shell element) also requires multiple elements to get good results. The comparison permits to verify rapid convergence of the proposed element. This test proves that the presented formulation takes the initial non-planar configuration of the beam into account properly.

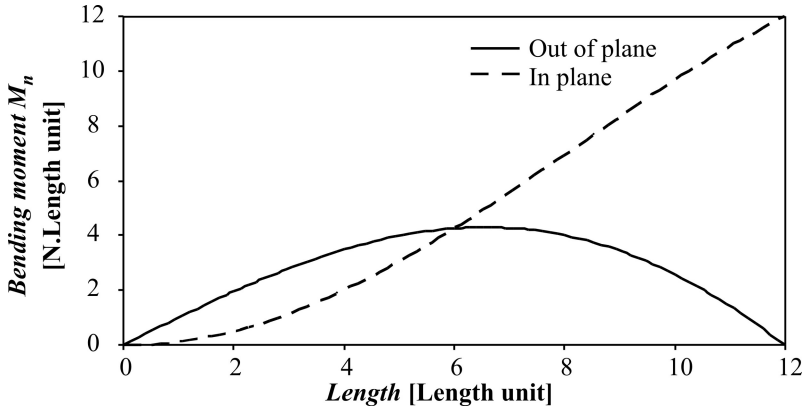


Fig. 5. Distribution of the module of the bending moment $M_{\mathrm{n}}$.

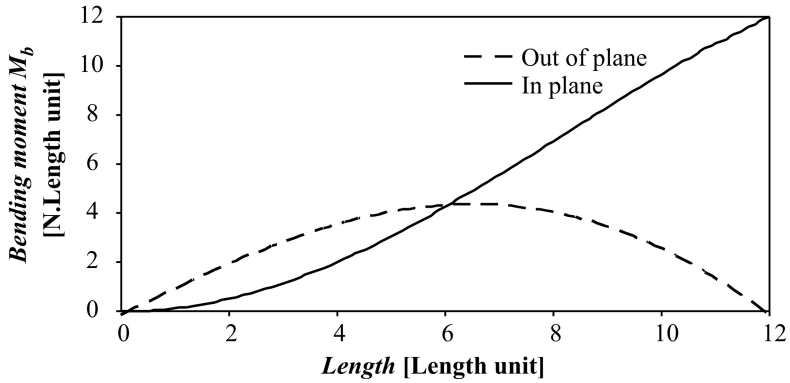


Fig. 6. Distribution of the module of the bending moment $M_{\mathrm{b}}$.

*Example 2: Simo test*

In this example, a problem studied by Simo et al. [28] is treated: it is similar to MacNeal and Harder test but it is a more demanding thin shell version: the thickness of the beam is changed only to be equal to 0.05. Simo et al. [28] calculated the analytical in-plane and out-of-plane deflections of the beam. Results given by different methods of modelling of this problem, among those given by the developed element, are presented in Table 2. The developed element gives results similar to others given by different methods, not only for in-plane and out-of-plane deflections, but also other displacements of the free end, which confirm the accuracy of the element, which simulates the total three-dimensional behaviour of the pre-twisted beam.

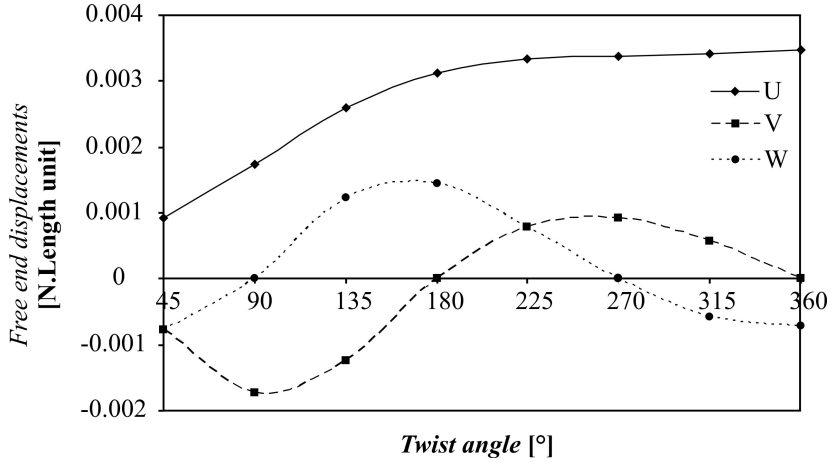


Fig. 7. Variation of free end displacements according the free-end twist angle.

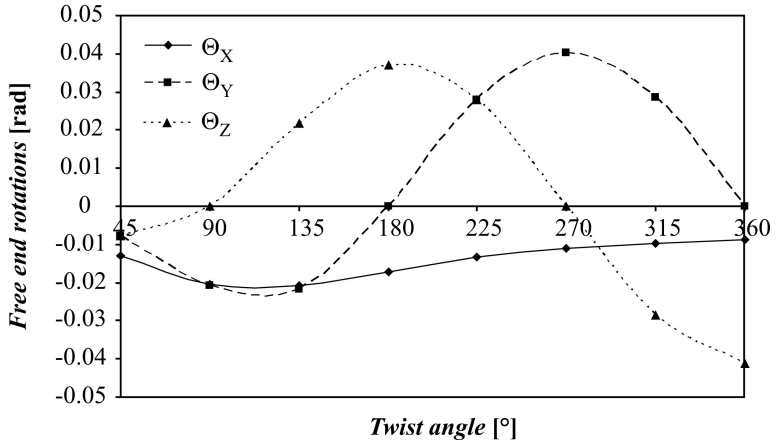


Fig. 8. Variation of free end rotations according the free-end twist angle.

*Example 3: Distribution of resulting forces*

In this study, we are interested to determine the distribution of different resulting forces along the beam for the MacNeal and Harder problem. Figures 3, 4, 5 and 6 present the module of these forces in two cases of load according to the length of the beam. These graphs reveal the similarity between the same resulting forces and others: this similarity is explained by the symmetric form of the beam

under consideration in the case of a total free-end twist angle equal to $\pi/2$. Values of all resulting forces on each beam extremity are equal to those of a non-twisted cantilever beam subjected to a unit load concentrated at the free end, but along the beam its form is non-linear, in fact, this form is due to the influence of the twist-angle presented in expressions of local base vectors (1–3): this influence is made through the $\cos\theta$ and $\sin\theta$. Bending moment $M_{\mathrm{n}}$ in the in-plane case and the bending moment $M_{\mathrm{b}}$ in the out-of-plane case present their maximum at the middle of the beam: this is due to the effect of the twist angle at this position ($\theta = \pi/4$) in which $\cos\theta = \sin\theta = \sqrt{1/2}$.

*Example 4: Influence of the free end twist angle*

This example is a study of the influence of the free-end twist angle on different displacements of the free end of the cantilever twisted beam as well as on the bending behaviour of the beam. Mechanical and geometrical properties of the studied beam are the same as in the MacNeal and Harder example, only the free end twist angle changes. We consider the case of a unit load in the $X$-axis direction, which is applied at the beam free end. Figures 7 and 8 present respectively free end displacements and rotations according to the free-end twist angle. We can observe an increase of the displacement $U$ along $X$ axis, other displacements ($V$ and $W$) decrease when the free-end twist angle increases. These graphs confirm the results of Zupan and Saje [39]: the more the free-end twist angle is increased, the more the structure becomes rigid in the $Y$ direction, and the more the beam becomes flexible in the $X$ direction.

## 5. Conclusion

In this paper a mixed-hybrid finite element for the pre-twisted beam modelling has been proposed. In the development of this element, the mixed-hybrid formulation is used and equilibrium equations are exactly satisfied. It has been shown that the present element leads to a good solution even with one element. Resulting forces along the beam are presented for different cases of loadings. An influence of the free-end twist angle is studied; the dependence of the rigidity of the structure on this angle is shown. This work opens perspectives for the study of other aspects in the twisted beam, like the study of the stress distribution along the structure.

## REFERENCES

[1] WASHIZU, K.: J. Math. Phys., *43*, 1964, p. 11.
[2] AIMIN, Y.—MINGXIA, F.—XING, M.: Comput. Struct., *80*, 2002, p. 2529.
[3] YU, A. M.—YANG, X. G.—NIE, G. H.: Int. J. Sol. Struct., *43*, 2006, p. 2853.
[4] AREISA, P. M. A.—SONG, J. H.—BELYTSCHKO, T.: Int. J. Num. Meth. Engrg., *64*, 2005, p. 1166.

[5] ASKU, T.: Comput. Struct., *57*, 1995, p. 973.
[6] AYAD, R.—RIGOLOT, A.: In : Proceedings of the 16$^{\text{éme}}$ Congrès Français de Mécanique, Nice 1–5 September 2003, p. 1.
[7] BELYTSCHKO, T.: Comput. Meth. Appl. Mech. Engrg., *96*, 1992, p. 93.
[8] BELYTSCHKO, T.—LEVIATHAN, I.: Meth. Appl. Mech. Engrg., *113*, 1994, p. 321.
[9] BELYTSCHKO, T.—WONG, B. L.—STOLARSKI, H.: Int. J. Num. Meth. Engrg., *28*, 1989, p. 358.
[10] DAMMAK, F.—ABID, S.—GAKWAYA, A.—DHATT, G.: Revue Européenne des éléments finis, *14*, 2005, p. 1.
[11] FISH, J.: Int. J. Num. Meth. Engrg., *33*, 1992, p. 149.
[12] GRUTTMANN, F.—WAGNER, W.: Comput. Meth. Appl. Mech. Engrg., *194*, 2005, p. 4279.
[13] GROENWOLD, A. A.— STANDER, N.: Engrg. Comput., *12*, 1995, p. 723.
[14] GÜZEY, S.—STOLARSKI, H. K.—COCHBURN, B.—TAMMA, K.: Comput. Meth. Appl. Mech. Engrg., *195*, 2006, p. 3528.
[15] IBRAHIMBEGOVIC, A.—FREY, F.: Int. J. Num. Meth. Engrg., *37*, 1994, p. 3659.
[16] JAMEI, S.—FREY, F.—JETTEUR, P.: Comput. Meth. Appl. Mech. Engrg., *75*, 1989, p. 251.
[17] JETTEUR, P.—FREY, F.: Engrg. Comput., *3*, 1986, p. 276.
[18] LIU, J.—RIGGS, R. H.—TISSLER, A.: Int. J. Num. Meth. Engrg., *49*, 2000, p. 1065.
[19] MacNEAL, R. H.—HARDER, R. L.: Finite Elements Anal. Des., *1*, 1985, p. 3.
[20] NAGANARAYANA, B. P.—PRATHAP, G.: Comput. Struct., *33*, 1989, p. 1107.
[21] PARK, D. W.—OH, S. I.: Comp. Meth. Appl. Mech. Engrg., *193*, 2004, p. 2105.
[22] SALEEB, A. F.—CHANG, T. Y.—GRAF, W.: Comput. Struct., *26*, 1987, p. 787.
[23] SAUER, R.: Bericht 4 (1998). Institut für Baustatik, Universität Karlsruhe (TH).
[24] SZE, K. Y: Comp. Meth. Appl. Mech. Engrg., *117*, 1994, p. 361.
[25] SZE, K. Y.—ZHU, Y.: Comp. Meth. Appl. Mech. Engrg., *174*, 1999, p. 57.
[26] TAYLOR, R. L.: Finite element analysis of linear shell problems. J. R. Whiteman Edition. The mathematics of finite elements and applications VI. London, Academic Press Ltd 1988, p. 191.
[27] ZHU, Y.—ZACHAIRA, T.: Comp. Meth. Appl. Mech. Engrg., *136*, 1996, p. 165.
[28] SIMO, J. S.—FOX, D. D.—RIFAI, M. S.: Comp. Meth. Appl. Mech. Engrg., *73*, 1989, p. 53.
[29] BASSAYA, K.—SHIRIMAVASA, V.: Comput. Struct., *74*, 2000, p. 167.
[30] HU, Y. K.—NAGY, L. I.: Comput. Struct., *65*, 1997, p. 893.
[31] LO, S. H.—LING, C.: Comp. Meth. Appl. Mech. Engrg., *189*, 2000, p. 961.
[32] MIJUCA, D.: The scientific journal FACTA UNIVERSITATIS. Series: Mechanics, Automatic Control and Robotics, *3*, 2001, p. 167.
[33] MIJUCA, D.: Comput. Mech., *33*, 2004, p. 466.
[34] SZE, K. Y.—YI, S.—TAY, M. H.: Int. J. Num. Meth. Engrg., *40*, 1997, p. 1839.
[35] SZE, K. Y.—YAO, L. Q.—PIAN, T. H. H.: Finite elements Anal. Des., *38*, 2002, p. 353.
[36] WAGNER, W.—KLINKEL, S.—GRUTTMAN, F.: Comput. Struct., *80*, 2002, p. 857.
[37] DUTTA, A.—WHITE, D. W.: Comput. Struct., *45*, 1992, p. 9.
[38] ZUPAN, D.—SAJE, M.: Comput. Model. Engrg. Sci., *4*, 2003, p. 301.
[39] ZUPAN, D.—SAJE, M.: Comput. Struct., *81*, 2003, p. 1875.
[40] ZUPAN, D.—SAJE, M.: Comp. Meth. Appl. Mech. Engrg., *192*, 2003, p. 5209.

[41] TAKTAK, M.—DAMMAK, F.—ABID, S.—HADDAR, M.: Int. J. Mech. Sci., *47*, 2005, p. 209.
[42] DAMMAK, F.—TAKTAK, M.—ABID, S.—HADDAR, M.: Eur. J. Mech. A/Solids, *24*, 2005, p. 1068.
[43] BOUABDALLAH, S.: Modélisation des coques cylindriques raidies, isotropes et composites. [Thesis de Doctorat]. Université de Technologie de Compiègne 1992.
[44] BATOZ, J. L.—DHATT, G.: Modélisation des structures par éléments finis. Volume 2, poutres et plaques. Paris, Edition Hermes 1990.

*Received: 22.10.2007*
*Revised: 7.7.2008*